Available online at www.sciencedirect.com
SCIENCE DIRECT
Polymer 46 (2005) 6513–6521
polymer
www.elsevier.com/locate/polymer

Study of the time evolution of the surface morphology of thin asymmetric diblock copolymer films under solvent vapor

Junchai Zhao, Shichun Jiang*, Xiangling Ji, Lijia An, Bingzheng Jiang

State Key Laboratory of Polymer Physics and Chemistry, Changchun Institute of Applied Chemistry, Chinese Academy of Sciences, Changchun 130022, People's Republic of China

Received 9 November 2004; received in revised form 17 April 2005; accepted 12 May 2005
Available online 22 June 2005

Abstract

The time development of the surface morphology of asymmetric polystyrene-*b*-poly(4-vinylpyridine) (PS-*b*-P4VP) thin films 'annealing' in methanol vapor, a selective solvent for minority P4VP block, was investigated by atomic force microscopy(AFM). For PS-*b*-P4VP with cylindrical structure in bulk, as annealing time progressed, the surface morphology underwent structural transitions from featureless topography to hybrid morphology of cylindrical and spherical pits, to cylinders, to nanoscale depressions, back to cylinders again. The different film thickness made the number of the transitions observed, at any given annealing time, different. The thicker the film is the more transitions at a given annealing time can be observed. If the film was not thick enough, depressions appeared. For PS-*b*-P4VP with spherical structure in bulk, it displayed nanoscale depressions with the annealing time increasing. A possible mechanism of the transition of morphologies during solvent annealing was proposed.

Keywords: Asymmetric diblock copolymer films; Solvent annealing; Surface morphology

1. Introduction

The ability to self-assemble into high regular structures with mesoscopic length scales makes the diblock copolymers present an interesting class of materials for thin film technology [1,2]. In bulk, the interplay of the incompatibility between the different blocks, and the chemical bond between them, give rise to a variety of ordered microdomain structures in thermal equilibrium. However, when the block copolymers are confined into a thin film, the interactions with the boundaries influence the orientation and its morphology. Generally, the morphology of diblock copolymer thin films mainly depends on the film thickness, the interactions with the boundaries, and the incompatibility between the two blocks of the copolymer, which is usually characterized by a Flory–Huggins parameter.

In recent years, there are many literatures about studying the evolution and orientation of microstructures in thin films by applying external fields, such as electric fields [3,4], shear [5,6], temperature gradients [7], graphoepitaxy [8,9], chemically patterned substrates [10–13], controlled interfacial interactions [14,15] and so on. Solvent evaporation is also a strong and highly directional field. Making block copolymer thin films under various solvent evaporation conditions turned out to be a good way to manipulate the microstructures [16,17]. Kim and Libera [16,18] demonstrated that the rate of solvent evaporation from thin, solution-cast block copolymer films can be used to manipulate the orientation of copolymer assemblies. Hahm et al. [19] and Kimura et al. [20] have also shown that evaporation-induced flow in solvent-cast block copolymer films can produce ordered arrays of nanoscopic cylindrical domains with a highly in-plan orientation and lateral order. Fukunaga et al. [17,21] recently showed that solvent annealing can greatly enhance the ordering of copolymer morphologies in very thin films. The simple process of solvent evaporation can also produce highly ordered arrays of cylindrical microdomains in block copolymers with long-range lateral order [22]. Recently, using solvent annealing, it was also shown that from a destabilization of confined films, nanostructured polymeric surfaces resulted as well [23–25].

* Corresponding author. Tel.: +86 431 5262138; fax: +86 431 5262126.
E-mail address: scjiang@ciac.jl.cn (S. Jiang).

0032-3861/$ - see front matter © 2005 Elsevier Ltd. All rights reserved.
doi:10.1016/j.polymer.2005.05.070

Solvent evaporation presents a simple route not only in controlling the alignment of the microdomain morphology, but also in varying the morphology of block copolymer. When the samples are exposed to solvent vapor, the mobility is imparted to the system, as when the polymer is heated above its T_g, and the morphology will change. Therefore, it is interesting to investigate the process of morphology evolution under various solvent vapors.

From the literature about solvent evaporation, it can be seen that most of the work has been done intensively on triblock copolymer [16,17,21,26–28]. In contrast, less work has been reported for symmetric [29] and asymmetric diblock copolymer thin films [30]. Therefore, it is worthwhile to study the fascinating phase behavior of diblock copolymer under solvent annealing. Presently, the development of surface morphology of asymmetric PS-*b*-P4VP (not very high molecular weight) under solvent vapor has been investigated in detail.

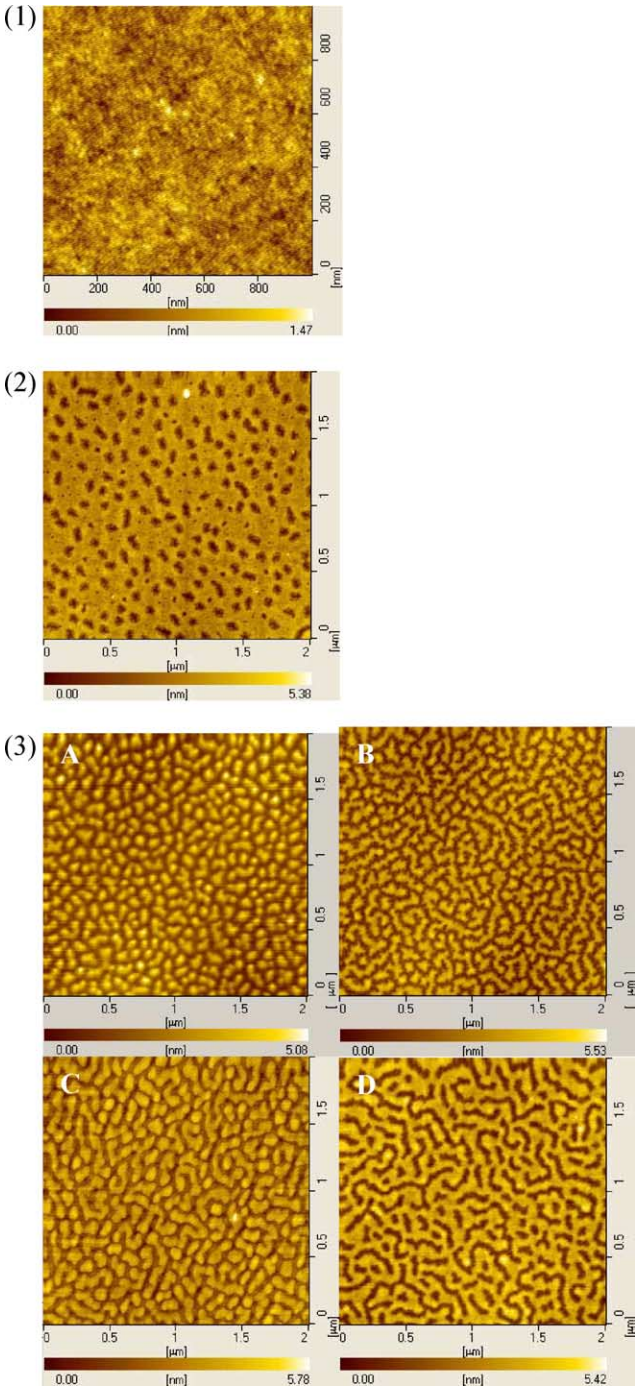

Fig. 1. (1) AFM topography of 19 nm asymmetric PS(40,000)-*b*-P4VP(5600) thin film after exposing to toluene vapor for 12 h. Image size: 1×1 μm^2. (2) AFM topography of 11 nm asymmetric PS(40,000)-*b*-P4VP(5600) thin film after exposing to toluene vapor for 12 h. Image size: 2×2 μm^2. (3) AFM topography of 6 nm asymmetric PS(40,000)-*b*-P4VP(5600) thin film after exposing to toluene vapor for (A) 0 h (B) 4 h (C) 8 h (D) 12 h. Image size: 2×2 μm^2.

2. Experimental section

2.1. Sample preparation

The asymmetric PS-*b*-P4VP diblock copolymers used in this study were obtained from Polymer Source Inc., with number molecular weight M_n of 31,900–13,200 and 40,000–5600 and polydispersity index $M_w/M_n = 1.08$ and 1.09, respectively.

PS-*b*-P4VP (40,000–5600) was dissolved in chloroform to form solutions with three different concentrations (0.05, 0.2, and 2 mg/mL). After spin-coating each solution onto cleaved mica surface at 3500 rpm for 30 s, three different film thickness ($\sim$6, $\sim$11, and $\sim$19 nm) were produced, which corresponded to the three different concentrations (0.05, 0.2, and 2 mg/mL), respectively. PS-*b*-P4VP (31,900–13,200) was also dissolved in chloroform to form solutions with three different concentrations (1, 2, and 5 mg/mL). The average thickness of the produced films from each solution was about 20, 35, and 78 nm, respectively. All the prepared films were dried in a desiccator at least for 4 h, and then they were placed into a glass vessel with 70 mL of the reservoir solvent at the initiation of the solvent annealing process. The temperature of the solvent vapor was kept at room temperature. After being exposed for different times to different solvent vapor, the samples were removed from the vessel and dried in the air at room temperature.

The film thickness was determined by D8 X-ray reflection (German) and AFM. For the AFM method, the sample was scratched and the height of the remaining polymer film was determined relative to the substrate.

2.2. Atomic force microscopy (AFM), X-ray photoelectron spectroscopy (XPS) and contact angle characterization

Surface morphologies of these samples were investigated by means of atomic force microscopy (SPI3800N, Seiko Instruments Inc., Japan), and the images were taken with the tapping mode.

The XPS was measured with VG ESCALAB MK at

room temperature by using an M_g K_α X-ray source ($h\nu$ = 1253.6 eV) at 14 kV and 20 mA. The X-ray beam was perpendicular incident to the sample surface in the measurement.

Contact angle measurements were performed with a KRÜSS DSA10-MK2 at an ambient temperature. The probe fluid used was deionized water with drop volumes of 1.5 μL.

3. Results and discussion

3.1. The morphologies of three thicknesses of PS(40,000)-b-P4VP(5600) thin films under two kinds of solvent vapor: toluene, a selective solvent for PS block; and methanol, a selective solvent for P4VP block

3.1.1. Toluene vapor

The film morphologies of three thicknesses, after treatment in toluene vapor, for different times are shown in Fig. 1. Whether annealed in toluene vapor for 4, 8 or 12 h, the 19 nm film always displayed a featureless morphology, just like the as-cast film. Here, the morphology after annealing for 12 h was given in Fig. 1(1). This phenomenon can be explained as follows: during toluene annealing, PS blocks adsorbed more toluene than P4VP due to the selective solvent of toluene for PS blocks. Hence, the mobility of PS was larger than that of P4VP. The smaller surface energy of PS (γ = 45.5 mJ/m^2) than P4VP (γ = 50.0 mJ/m^2) [31] made PS blocks tend to move towards the air surface. In addition, the attraction between PS and toluene was also favorable for PS exposing to the air surface. Based on these facts, there was more PS located at the air surface after treatment, and the film exhibited featureless the whole time. The water contact angle was larger than that of the as-cast sample, which again confirmed that more PS block enriched at the surface after treatment.

This phenomenon of planarization can also be explained as an interfacial behavior. In the solvent-annealing chamber the film is in contact with an air/solvent mixture that has higher surface tension than air. When the film is brought out of the chamber to solvent-free air, the film/air interfacial tension abruptly increases, and the surface undulation is produced. The undulations can be dampened by increasing the thickness of the surface layer and diffusing more PS from the 'interior' area to the surface [32].

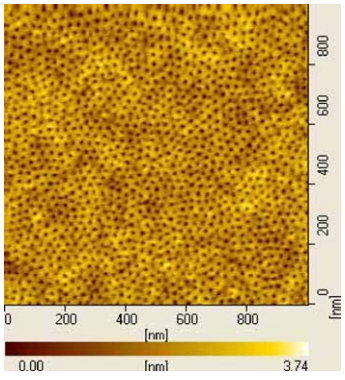

Fig. 2. AFM topography of 19 nm asymmetric PS(40,000)-*b*-P4VP(5600) thin film after exposing to methanol vapor for 144 h.

However, for the 11 nm film (Fig. 1(2)), it was not the case. As-cast sample showed a featureless morphology. After annealing in toluene vapor for 4 h, pits distributed in a disordered state covered the whole surface. After 8 and 12 h, the morphology still remained pits, but the size became slightly larger. Here, the surface morphology after annealing for 12 h under toluene vapor was given.

The as-cast sample of 6 nm film displayed short strips. After treatment in toluene vapor for 4 h, cylindrical structures appeared. After 8 h the cylinder became wider, at the same time the distance between them also became smaller. After 12 h, strip-like corrugations appeared. It can be seen from Fig. 1(3). For 6 nm film, under toluene vapor, the mobility of polymer chains improved, causing the smaller strips gradually to move together and congregate into cylinders.

3.1.2. Methanol vapor

Because methanol is a selective solvent for P4VP block, P4VP blocks would absorb more methanol than PS during solvent annealing. After drying, PS block would be higher than P4VP due to solidifying first.

For 19 nm film, the surface of as-cast sample was featureless. However, after treatment in methanol vapor for various times (4, 8, 12, 24, 48, 72, 144 h), it always behaved a hexagonally-arranged nanoscale depression (the morphology after annealing for 144 h was given in Fig. 2). That is to say, once this morphology was formed, it would have nothing to do with the annealing time.

For 11 nm film, after annealing for different times (4 or 8 or 12 h), it was only the case that pits were distributed in a disordered state on the surface, like Fig. 1(2).

For 6 nm film, short strips appeared after annealing in methanol vapor for 4 h. After 8 h, the short strips gradually merged to form cylinders because of the improved mobility, and reconstruction occurred.

From Figs. 1 and 2, hexagonal nanostructures can be found in the thicker film (~19 nm) after treatment in methanol vapor. Moreover, this structure does not vary with the annealing time. For moderate thicker film (~11 nm), only disordered pits can be observed. For the thinner film (~6 nm), no matter what the selective solvent vapor for PS or for P4VP, the solvent can impart substantial mobilities to the whole film due to the thin of the film. Reconstruction can be realized, and the cylinder formed.

3.2. Development of morphology of asymmetric PS-b-P4VP with cylindrical structure in bulk under methanol vapor

From the above experiments, we knew that the thicker film (~19 nm) of PS-*b*-P4VP with spherical structure in bulk can form ordered structures after treatment in methanol

vapor. Therefore, the evolution of the surface morphology of thicker film (>19 nm) of PS-*b*-P4VP with cylindrical structure in bulk under methanol vapor was investigated in the following.

It is well known that morphology and orientation of domains in cylinder and lamella forming diblock copolymers could be successfully controlled by using external fields such as electrical fields [3,33] and surface interactions [34–37]. As the method of surface interactions, for a specific A–B diblock copolymer, the surface energies of the components, σ_A and σ_B, and the segmental interaction parameter χ_{AB} are dictated by the chemical composition of the copolymer, and they are invariant. The fundamental period of the copolymer is also fixed, the film thickness of a specimen can be known as well after preparation. This leaves the interfacial energy between the components and the substrates, γ_{AS} and γ_{BS} as the only variables [38]. Hence, by varying the two parameters, the morphology can be controlled easily.

The morphologies of polymer films with different thickness, or with the same thickness but different annealing time are investigated. First, we observed the evolution of the morphology of 20 nm film under methanol vapor. The as-cast film was featureless, but it was found that pits distributed in disorder were full of the surface after annealing for each different time (4, 8, 12, 24, 48, and 108 h). The morphology after treatment for 108 h was shown in Fig. 3. Fig. 4 depicts the development of morphology of 35 nm film under methanol vapor, topographic and phase images were all given. It was seen that the surface of as-cast sample was featureless, but after 4 h annealing, the hybrid structure consisting of cylindrical and spherical pits appeared on the surface. After 8 h, cylindrical structure became more and more. When annealing time was 12 h, cylindrical structure reached the most. Continued annealing to 16 h, some pits were observed. After 20 h, pits became dominant. After this, the structure no longer changed with annealing time increasing, which can be seen from the morphologies obtained after treatment in vapor for 27, 48, 72, and 144 h (Fig. 4(G)–(J)). It can be said that the structure with more pits and few cylinders was the equilibrium morphology. Similar to 35 nm film, the 78 nm film also underwent a serial of morphological transitions, its topographic and phase images are all shown in Fig. 5. From Fig. 5 we can see that the as-cast sample was also uncharacteristic. After 4 h annealing, hybrid structure with cylindrical and spherical pits appeared. After 24 h, the whole surface was full of cylinders. But when the annealing time increased to 48 h, well-ordered nanoscale depressions were observed. Continued annealing to 60 h, nanoscale depressions became unclear. After 72 h, cylindrical channels appeared. When annealing time was 84 and 96 h, cylinders became dominant again. After 144 h, long and

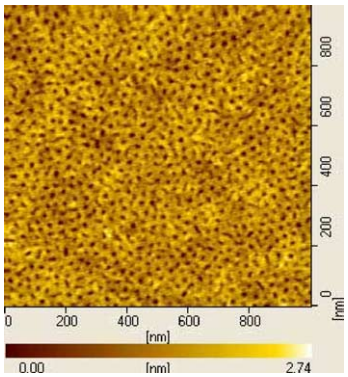

Fig. 3. AFM topography of 20 nm asymmetric PS(31,900)-*b*-P4VP(13,200) thin film after annealing in methanol vapor for 108 h.

extended cylinders were distributed all over the surface, and at 192 h it still presented cylindrical structures. It also can be said that the equilibrium morphology cylinders existed after 144 h annealing.

From Figs. 3–5, it can be concluded that the observed transitions were strongly dependent on the film thickness. The thicker the film is, the more transitions would be seen, but if the film is very thin, only pits can be observed.

A mechanism of solvent annealing for asymmetric PS-*b*-P4VP with cylindrical structure in bulk was shown in Fig. 6. Fig. 6(1) showed the model of time development of morphology of thinner asymmetric PS-*b*-P4VP film under methanol vapor. The as-cast surface was featureless (Fig. 6(1a)). When exposed to methanol vapor, the attraction between the P4VP and methanol made P4VP move towards the free surface. However, the repulsion between the PS and methanol made PS move towards substrate. So, depressions appeared on the surface after drying (Fig. 6(1b)), moreover, in the whole annealing process only this structure was observed. It was considered that when annealing, not many P4VP blocks in this thin film would move towards the surface early. Due to the fewer P4VP blocks compared to the thicker film, only pits were observed.

For the thicker film (Fig. 6(2)), the appearance of the hybrid structure (Fig. 6(2a)) was explained as following: the surface of as-cast samples was featureless, and the thickness was undulate. However, in the interior various orientations of cylinders existed. The parallel cylinder corresponded to the high part of the surface, while the perpendicular cylinder corresponded to the low part of the surface. Thus, high parts were thick and low parts were thin. The reason for saying so was that for the thinner part of the film, in order to reduce the total free energy, the orientation of cylinders perpendicular to the surface must be taken, so that the equilibrium repeat distance can be maintained [39]. Methanol was a selective solvent for P4VP, after treatment in methanol vapor for 4 h, the hybrid structure of cylindrical (parallel

Fig. 4. AFM topographic (left) and phase images (right) of 35 nm asymmetric PS(31,900)-*b*-P4VP(13,200) thin films after annealing in methanol vapor for different times (A) 0 h (B) 4 h (C) 8 h (D) 12 h (E) 16 h (F) 20 h (G) 27 h (H) 48 h (I) 72 h (J) 144 h.

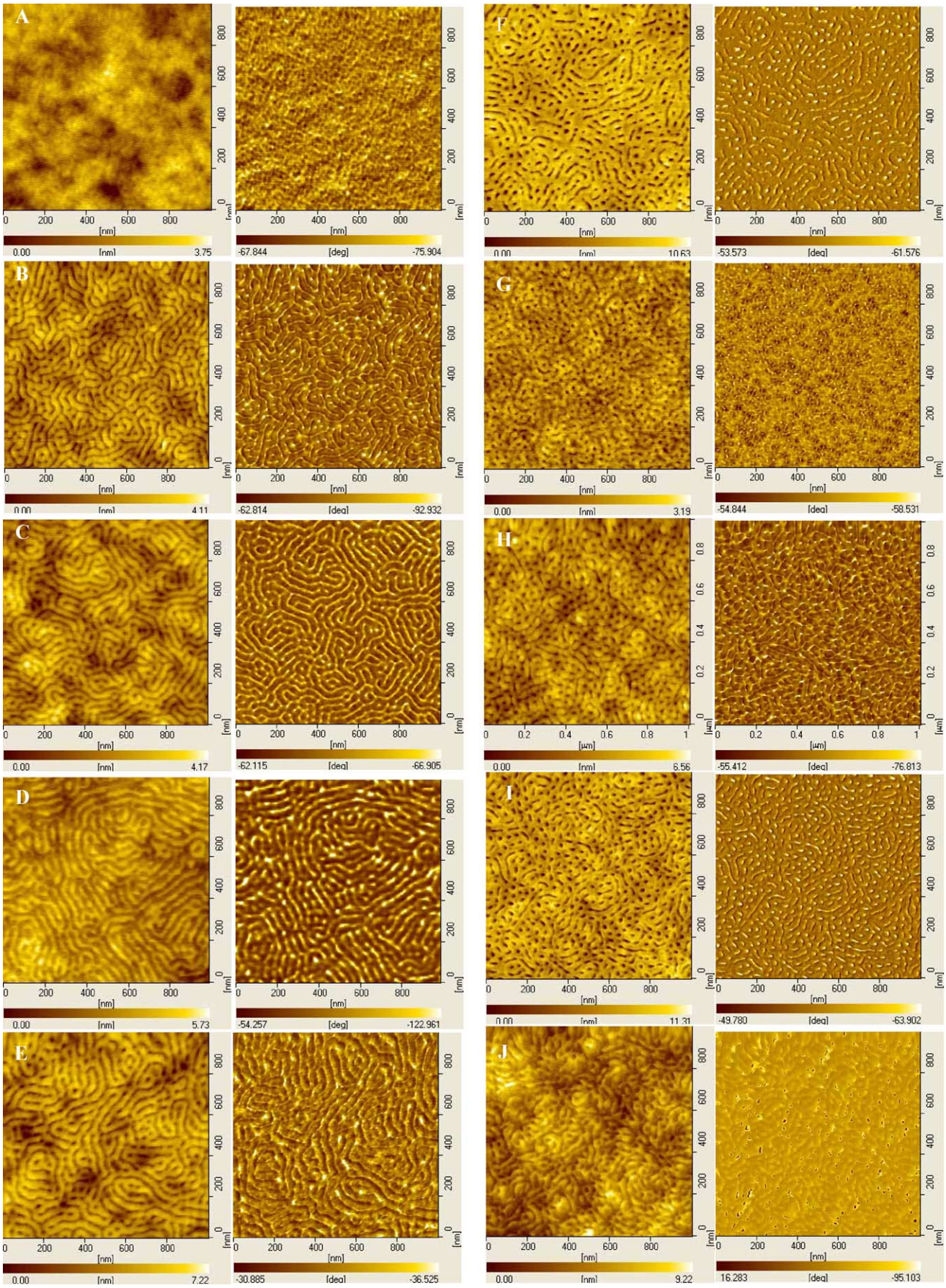
A
0.00 [nm] 3.75
-67.844 [deg] -75.904
B
0.00 [nm] 4.11
-62.814 [deg] -92.932
C
0.00 [nm] 4.17
-62.115 [deg] -66.905
D
0.00 [nm] 5.73
-54.257 [deg] -122.961
E
0.00 [nm] 7.22
-30.885 [deg] -36.525
F
0.00 [nm] 10.63
-53.573 [deg] -61.576
G
0.00 [nm] 3.19
-54.844 [deg] -58.531
H
0.00 [nm] 6.56
-55.412 [deg] -76.813
I
0.00 [nm] 11.31
-49.780 [deg] -63.902
J
0.00 [nm] 9.22
16.283 [deg] -95.103

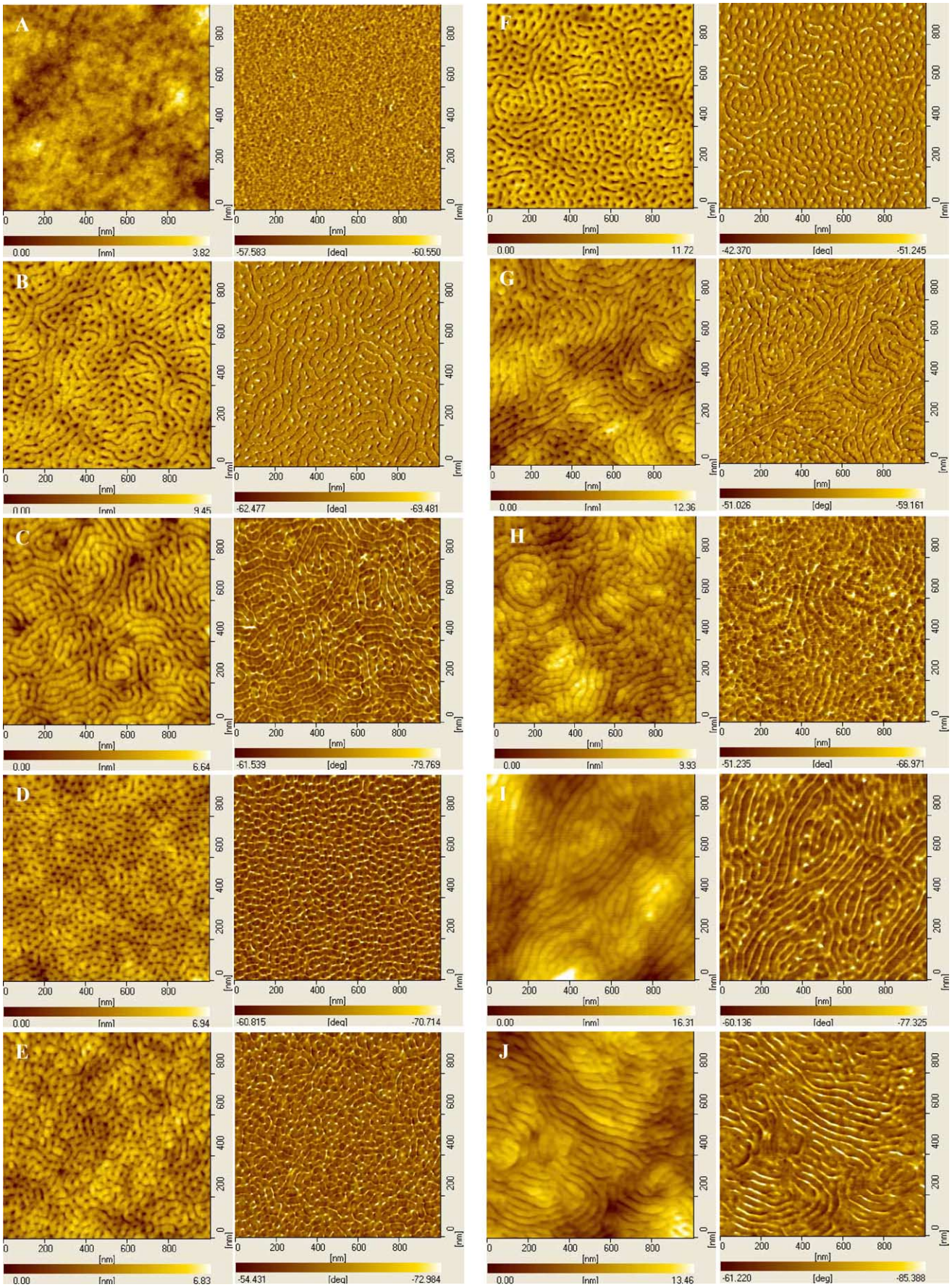
A
0 200 400 600 800 [nm]
0.00 [nm] 3.82
-57.583 [deg] -60.550
B
0.00 [nm] 9.45
-62.477 [deg] -63.481
C
0.00 [nm] 6.64
-61.539 [deg] -79.769
D
0.00 [nm] 6.94
-60.815 [deg] -70.714
E
0.00 [nm] 6.83
-54.431 [deg] -72.984
F
0.00 [nm] 11.72
-42.370 [deg] -51.245
G
0.00 [nm] 12.36
-51.026 [deg] -59.161
H
0.00 [nm] 9.93
-51.235 [deg] -66.971
I
0.00 [nm] 16.31
-60.136 [deg] -77.325
J
0.00 [nm] 13.46
-61.220 [deg] -85.388

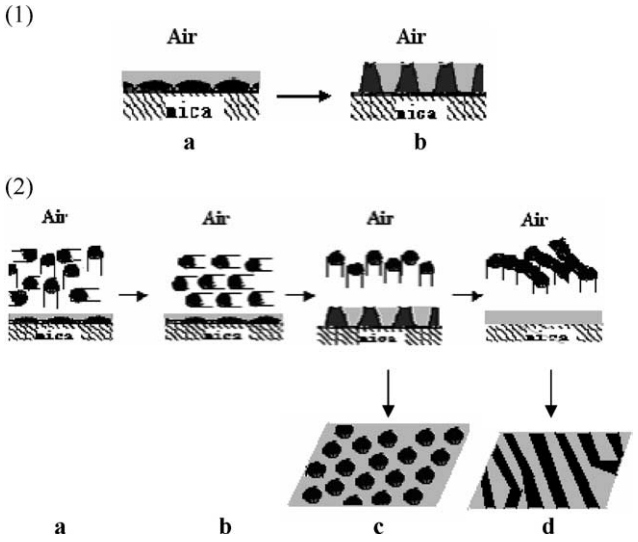

Fig. 6. Schematic model of time development of morphology of thin asymmetric PS(31,900)-*b*-P4VP(13,200) film under methanol vapor(shown as cross-section view). The black regions denote P4VP, and the gray areas denote PS, (1) thinner film, (2) thicker film (to c and d, plane views were also given under the cross-section sketch map).

cylinders formed) and spherical pits (perpendicular cylinders formed) were seen on the surface. As annealing time progressed, the mobility of polymer chains increased further, making the randomly orientational domains ordered (Fig. 6(2b)). Moreover, it was possible that the system still behaved asymmetric wetting at this moment, and parallel structure was also favorable in this case. So the parallel cylinders full of the surface were seen (Figs. 5(c) and 6(2b)). As annealing time increased, perpendicular cylinders were seen (Fig. 6(2c)). We know, when film was exposed to the methanol vapor, the solvent could mediate interactions between the segments of the copolymer, reducing differences in the surface energies of the components [20]. In addition, van der Waals interaction between polymer molecules and the substrate is also markedly changed by the incorporated solvent molecules [40]. Hence, it was possible that as annealing time increased, more and more P4VP blocks would flee from the bondage of the substrate. It can be imaged that at a certain time the neutral surface could be formed and the asymmetric wetting also became the symmetric wetting because of the migration of P4VP block to the air surface. Once the neutral surface appeared, the perpendicular cylinder would be observed. Since, the film was exposed to the selective solvent for P4VP, on the surface, it would appear nanoscale depressions. Results presented in Figs. 4(G) and 5(D) were in accord with our analysis. With further annealing, a second cylindrical structure was full of surface (Figs. 5(I) and 6(2d)). With prolonged exposure to methanol vapor more and more P4VP migrated to the air surface, nanoscale depressions

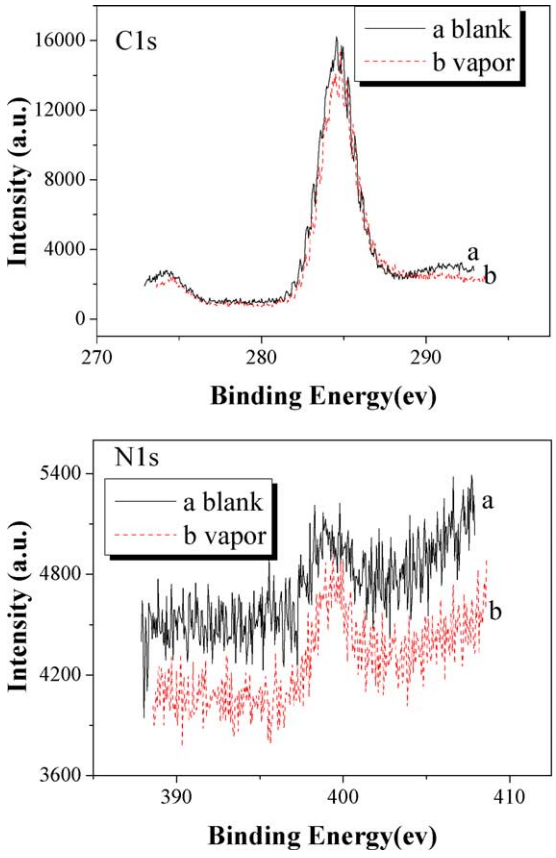

Fig. 7. XPS spectrum in the C1s and N1s regions, (a) for the original film (sample of Fig. 5(A)), (b) after treatment in methanol vapor for 144 h (sample of Fig. 5(I)).

began to connect each other and formed cylindrical channels. This morphology can also be considered as cylinders. With the extended annealing to 192 h (Fig. 5(J)), the morphology still behaved cylinder. It was considered that it reached a kind of equilibrium after 144 h annealing, and at the moment P4VP blocks may be completely migrate to the air surface, asymmetric wetting occurred again. It also can be seen from the fact that the surface area covered by P4VP blocks (60.1%) was larger than that of PS blocks (39.9%) when the final morphology was formed.

The second cylindrical structure could not be observed in 35 nm film (Fig. 4). The reason was the same as that of the thinner film (~20 nm).

To characterize the wettability of the surface after treatment in methanol vapor, XPS and contact angle experiments were performed. The experimental results of the samples of Fig. 5(A) and (G) are presented in Fig. 7, Tables 1 and 2. From Fig. 7 and Table 1, it was seen that after treatment in methanol vapor for 144 h, the carbon concentration decreased on the surface, comparable to the samples without annealing, but the nitrogen concentration increased. The result of contact angle measurement

Fig. 5. AFM topographic (left) and phase images (right) of 78 nm asymmetric PS(31,900)-*b*-P4VP(13,200) thin films after annealing in methanol vapor for different times (A) 0 h (B) 4 h (C) 24 h (D) 48 h (E) 60 h (F) 72 h (G) 84 h (H) 96 h (I) 144 h (J) 192 h.

Table 1
Surface composition measured by XPS

Atomic concentration	C (%)	N (%)
Without treatment (Fig. 5(A))	98.53	1.47
After treatment in methanol vapor for 144 h (Fig. 5(I))	97.43	2.57

(Table 2) indicated that the water contact angle of PS-*b*-P4VP film without treatment was almost equal to that of pure PS [41], which indicated that the surface of the original PS-*b*-P4VP film was covered by PS blocks and after treatment the water contact angle of PS-*b*-P4VP film was smaller than that of the samples without annealing. During annealing, we also have ever measured some water contact angle of the films annealed in different time and found that on the whole water contact angle of the films decreased with the annealing time increasing. But when the morphology gradually approached to the equilibrium structure, the change of the contact angle became smaller and smaller. Both XPS and contact angle results demonstrated that more P4VP migrated to the surface after treatment in methanol vapor, at the same time the surface behaved more hydrophilic. That is to say, surface chemical component and surface microstructure were the two main factors that contributed to the change of the surface wettability [42].

3.3. Development of morphology of asymmetric PS-b-P4VP thin film with spherical structure in bulk

For asymmetric PS(40,000)-*b*-P4VP(5600) (~19 nm) with spherical structure in bulk, the low content of P4VP blocks in the diblock copolymer made only one kind of structure nanoscale depression observed in the whole annealing process (Fig. 2). A schematic model for time development of morphology of this thin film under methanol vapor is shown in Fig. 8. The surface of an as-cast sample also displayed featurelessness, but the interior of the film existed spherical domains with various orientations (Fig. 8(a)). When exposed to methanol vapor, the attraction between the P4VP and methanol made P4VP move towards the free surface. However, the repulsion between the PS and methanol made PS move towards the substrate. Moreover, during solvent annealing the interior domains also underwent ordering. So after drying, well-ordered hexagonally packed nanoscale depressions were observed (Figs. 2 and 8(b) and (c)).

Table 2
Water contact angles for the pure PS and the samples shown in Fig. 5(A) and (I)

Sample	Average contact angle (°)
Pure PS	89.0
Without treatment (Fig. 5(A))	89.8±1.0
After treatment in methanol vapor for 144 h (Fig. 5(I))	69.4±1.5

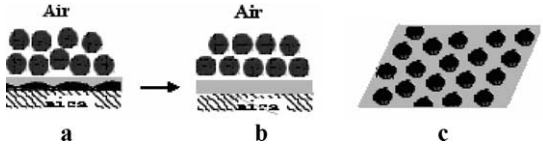

Fig. 8. Schematic model of time development of morphology of thin asymmetric PS(40,000)-*b*-P4VP(5600) film under methanol vapor. The black regions denote P4VP, and the gray areas denote PS, a and b are cross-section views and c is a plane view of b.

4. Conclusions

Asymmetric PS-*b*-P4VP thin films displayed plentiful morphologies under methanol vapor, a selective solvent for minority P4VP block. For PS-*b*-P4VP with cylindrical structure in bulk, as annealing time progressed, the surface morphology underwent structural transitions from a featureless surface, to a hybrid morphology of cylindrical and spherical pits, to cylinders, to nanoscale depressions, back to cylinders again. The number of transitions was determined by film thickness; the thicker the film is, the more transitions would be observed. If the film was not thick enough, only the pits were observed. For PS-*b*-P4VP with spherical structure in bulk, it only displayed well-ordered nanoscale depressions as the annealing time increased.

Acknowledgements

This work was supported by the National Natural Science Foundation of China for General (50303017, 50373044) and Major (20490220, 50390090), the Special Funds for Major State Basic Research Projects (No. 2003CB615600) and the Fund for Distinguished Young Scholars of China (No. 59825113) and the Chinese Academy of Sciences (KJCX2-SW-H07).

References

[1] Spatz JP, Eibeck P, Mößmer S, Möller M, Herzog T, Ziemann P. Adv Mater 1998;10:849.
[2] Thurn-Albrecht T, Steiner R, DeRouchey J, Stafford CM, Huang E, Bal M, et al. Adv Mater 2000;12:787.
[3] Morkved TL, Lu M, Urbas AM, Ehrichs EE, Jaeger HM, Mansky P, et al. Science 1996;273:931.
[4] Thurn-Albrecht T, Schotter J, Kästle GA, Emley N, Shibauchi T, Krusin-Elbaum L, et al. Science 2000;290:2126.
[5] Albalak RJ, Thomas EL, Capel MS. Polymer 1998;38:3819.
[6] Villar MA, Rueda DR, Ania F, Thomas EL. Polymer 2002;43:5139.
[7] Bodycomb J, Funaki Y, Kimishima K, Hashimoto T. Macromolecules 1999;32:2075.
[8] Segalman RA, Yokoyama H, Kramer EJ. Adv Mater 2001;13:1152.
[9] Cheng JY, Ross CA, Thomas EL, Smith HI, Vancso GJ. Appl Phys Lett 2002;81:3657.
[10] Fasolka MJ, Harris DJ, Mayes AM, Yoon M, Mochrie SGJ. Phys Rev Lett 1997;79:3018.
[11] Rockford L, Liu Y, Mansky P, Russell TP, Yoon M, Mochrie SGJ. Phys Rev Lett 1999;82:2602.

[12] Rockford L, Mochrie SGJ, Russell TP. Macromolecules 2001;34:1487.
[13] Kim SO, Solak HH, Stoykovich MP, Ferrier NJ, de Pablo JJ, Nealey PF. Nature 2003;424:411.
[14] Mansky P, Liu Y, Huang E, Russell TP, Hawker C. Science 1997;275:1458.
[15] Huang E, Rockford L, Russell TP, Hawker CJ. Nature 1998;395:757.
[16] Kim G, Libera M. Macromolecules 1998;31:2569.
[17] Fukunaga K, Elbs H, Magerle R, Krausch G. Macromolecules 2000;33:947.
[18] Kim G, Libera M. Macromolecules 1998;31:2670.
[19] Hahm J, Sibener SJ. Langmuir 2000;16:4766.
[20] Kimura M, Misner MJ, Xu T, Kim SH, Russell TP. Langmuir 2003;19:9910.
[21] Fukunaga K, Hashimoto T, Elbs H, Krausch G. Macromolecules 2002;35:4406.
[22] Kim SH, Misner MJ, Xu T, Kimura M, Russell TP. Adv Mater 2004;16:226.
[23] Müller-Buschbaum P, Gutmann JS, Stamm M, Cubitt R, Cunis S, von Krosigk G, et al. Phys B: Condens Matter 2000;283:53.
[24] Muller-Buschbaum P, Gutmann JS, Stamm M. Phys Chem Chem Phys 1999;1:3857.
[25] Müller-Buschbaum P, Gutmann JS, Cubitt R, Stamm M. Colloid Polym Sci 1999;277:1193.
[26] Zhang Q, Tsui OKC, Du B, Zhang F, Tang T, He T. Macromolecules 2000;33:9561.
[27] Elbs H, Drummer C, Abetz V, Krausch G. Macromolecules 2002;35:5570.
[28] Niu S, Saraf RF. Macromolecules 2003;36:2428.
[29] Xuan Y, Peng J, Cui L, Wang H, Li B, Han Y. Macromolecules 2004;37:7301.
[30] Chen Y, Huang H, Hu Z, He T. Langmuir 2004;20:3805.
[31] Sohn BH, Seo BW, Yoo SI, Zin WC. Langmuir 2002;18:10505.
[32] Saraf RF, Niu S, Stumb E. Appl Phys Lett 2002;80:4425.
[33] Mansky P, DeRouchey J, Russell TP, Mays J, Pitsikalis M, Morkved T, et al. Macromolecules 1998;31:4399.
[34] Huang E, Russell TP, Harrison C, Chaikin PM, Register RA, Hawker CJ, et al. Macromolecules 1998;31:7641.
[35] Mansky P, Russell TP, Hawker CJ, Pitsikalis M, Mays J. Macromolecules 1997;30:6810.
[36] Yang XM, Peters RD, Nealey PF, Solak HH, Cerrina F. Macromolecules 2000;33:9575.
[37] Peters RD, Yang XM, Nealey PF. Macromolecules 2002;35:1822.
[38] Russell TP, Thurn-Albrecht T, Tuominen M, Huang E, Hawker CJ. Macromol Symp 2000;159:77.
[39] Suh KY, Kim YS, Lee HH. J Chem Phys 1998;108:1253.
[40] Muller-Buschbaum P, Cubitt R, Petry W. Langmuir 2003;19:7778.
[41] Anastasiadis SH, Retsos H, Pispas S, Hadjichristidis N, Neophytides S. Macromolecules 2003;36:1994.
[42] Lei YG, Cheung ZL, Ng KM, Li L, Weng LT, Chan CM. Polymer 2003;44:3883.